

CLIMATIC PREDICTABILITY AND DYNAMICAL SYSTEMS

C. NICOLIS
Institut d'Aéronomie Spatiale de Belgique
Avenue Circulaire 3
1180 Bruxelles
Belgique.

ABSTRACT. The applications of the methods of dynamical systems to the analysis of climatic variability are discussed. Climatic change is viewed, successively, as the transition between multiple steady states, as the manifestation of sustained oscillations of the limit cycle type and as a non-periodic behavior associated to a chaotic attractor. A method to reconstruct the climatic attractor from time series data independent of any modelling is presented. The results suggest that long term climatic change is described by a chaotic attractor of low fractal dimensionality.

1. INTRODUCTION

In this chapter we attempt to clarify the relative role of internally generated and external mechanisms of climatic change. Much of our discussion will be concerned with long term problems and, in particular, with the quaternary glaciations. However, similar ideas and techniques could most certainly be applied to short and intermediate scale problems as well.

The classical tool of the paleoclimatologist is the analysis of variance spectra of various climatic indices, such as the oxygen isotope record of ice or deep sea core sediments^{1,2)} (Figs. 1 and 2). Although the importance of this tool should not be underestimated, we believe that it is essential to develop alternative methods. Indeed, besides allowing one to identify the characteristic time scales involved in a problem, spectral analysis gives only limited information on the nature of the underlying system, since it refers to gross, averaged properties. As a matter of fact a striking theorem proved recently³⁾ asserts that a power spectrum does not even allow one to differentiate between noisy or deterministic evolutions!

The approach we shall adopt is motivated by the concepts and techniques of the theory of nonlinear dynamical systems. At the basis of our analysis is the idea that climatic change reflects the ability of a certain dynamical system to undergo instabilities and transitions between different regimes. We will examine some typical

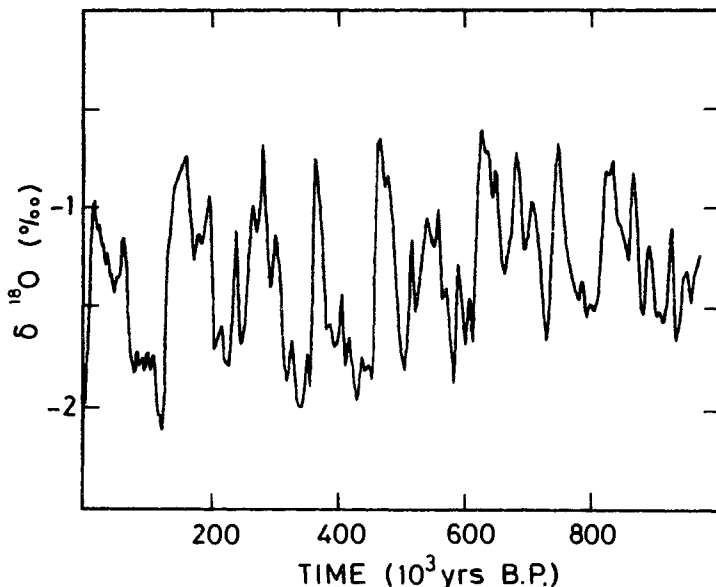


Fig. 1. Oxygen isotope record deduced from the V28238 deep sea core¹⁾.

scenarios of such transitions. We will also assess the role of external periodic perturbations, arising from the earth's orbital variations, or of internally generated fluctuations, on these transitions. Next, we will propose a new method of analysis of the climatic record based on developments of dynamical systems theory, which will allow us to actually identify the dynamical regime represented by the data. This conclusion will finally be confronted with the predictions of mathematical models.

2. CLIMATIC VARIABILITY VIEWED AS TRANSITION BETWEEN MULTIPLE STEADY STATES

As shown in the chapter by G. Nicolis⁴⁾, the simplest attractor representing the long term behavior of a dynamical system is the point attractor. If only one such attractor is available the system will end up in a unique stationary state, and the problem of variability simply will not arise. We therefore inquire, in this section, on the possibilities arising from the coexistence of multiple point attractors in climate dynamics.

Energy balance models, a class of climatic models treated more amply in the chapters by Ghil⁵⁾ and Saltzman⁶⁾, are known to generate quite naturally this behavior. To simplify matters as much

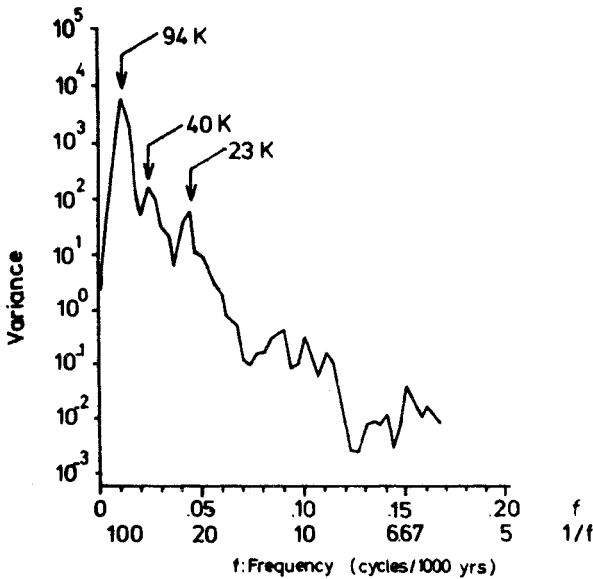


Fig. 2. Typical variance spectra deduced from the paleoclimatic record of the last million years.

as possible consider the case of globally averaged (also referred to as zero-dimensional 0-d) models :

$$\begin{aligned} \frac{dT}{dt} &= \frac{1}{C} \left\{ \left(\begin{array}{c} \text{incoming} \\ \text{solar energy} \end{array} \right) - \left(\begin{array}{c} \text{outgoing} \\ \text{infrared energy} \end{array} \right) \right\} \\ &= \frac{1}{C} [Q (1 - \alpha(T)) - \epsilon_B \sigma T^4] \end{aligned} \quad (1)$$

where T is the space averaged surface temperature, C the heat capacity, Q the solar constant, α the albedo, σ the Stefan constant and ϵ_B the emissivity factor representing the deviation from black body radiation. The surface-albedo feedback can be readily incorporated in this picture by modelling the albedo as a stepwise linear function⁷⁾. The resulting energy balance is represented in Fig. 3.

For plausible parameter values it can give rise to two stable steady states, T_a and T_b , representing respectively a glacial and a more favorable climate, separated by an intermediate unstable one, T_c . If (as suggested by the record) the difference $T_a - T_b$ is small, the system could be further assumed to operate near a pitch-

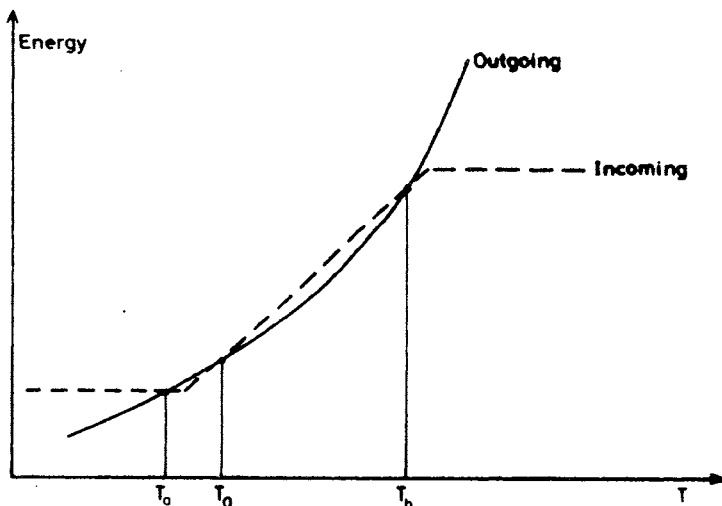


Fig. 3. Incoming and outgoing radiative energy curves as functions of T (global average temperature). Their intersections T_a , T_b and T_0 are the steady states predicted by eq. (1).

fork bifurcation point. As shown in the chapter by G. Nicolis, such a system can be brought to the following universal, normal form⁴⁾:

$$\frac{dx}{d\tau} = f(x, \lambda) = \lambda x - ux^3 \quad (2)$$

where x , τ , u and λ are appropriately scaled combinations of initial variables, time and parameters.

Whether viewed in the form of (1) or (2), climatic change necessitates a transition between states a and b . Now, in the model elaborated so far no mechanism allowing for such a transition is present except for the trivial one, whereby the system initially at T_b (say) is perturbed and brought near T_a . Such massive perturbations are however hard to imagine. We therefore enlarge now our description by incorporating the effect of random fluctuations $F(t)$ which, as explained in previous chapters, are always present in a complex physical system⁴⁾. We model these fluctuations as a Gaussian white noise⁸⁾:

$$\langle F(t) \rangle = 0$$

$$\langle F(t) F(t') \rangle = q \delta(t - t') \quad (3)$$

where q is the variance of fluctuations, and write the augmented energy balance equation as

$$\frac{dx}{d\tau} = f(x, \lambda) + g(x) F(\tau) \quad (4)$$

where $g(x)$ represents the coupling of the internal dynamics to $F(\tau)$.

This equation can be studied by the methods of the theory of stochastic processes. The main result is that the random forcing induces a diffusion-like motion between stable attractors which occurs on a time scale given by⁹⁾

$$\tau_{a,b} \sim \exp \left\{ \frac{2}{q} \Delta U_{a,b} \right\} \quad (5)$$

The quantity ΔU_a or ΔU_b is known as potential barrier. It is defined by

$$\Delta U_{a,b} = U_0 - U_{a,b} \quad (6a)$$

where U is the integral of the right hand side of eqs (1) or (2) :

$$U(x, \lambda) = - \int^x dx' f(x', \lambda) \quad (6b)$$

By analogy to mechanics U can be referred to as climatic potential, since its derivative $\partial U/\partial x$ represents the "force", f responsible for the evolution. If as expected the variance of the fluctuations q is small and the barrier ΔU finite, τ_a or τ_b will be much larger than the local relaxation time and could well be in the range of glaciation time scales⁹⁾. In contrast, the local evolution in the vicinity of each attractor is given by the inverse of the first derivative of f , evaluated on a or b . For an energy balance model it should be, typically, of the order of the year. Still, eq. (4) cannot be considered as a satisfactory model of quaternary glaciations : the transitions between a and b occur at randomly distributed times, whereas the climatic record suggests that quaternary glaciations have a cyclic character bearing some correlation with the mean periodicities of the earth's orbital variations. Let us therefore study the response of our multistable model to both stochastic and periodic perturbations. Taking the simplest case of a sinusoidal forcing one is led to

$$\frac{dx}{d\tau} = f(x, \lambda) + g(x) [\varepsilon \sin \omega \tau + F(\tau)] \quad (7)$$

where ε and ω are respectively the amplitude and frequency of the forcing. It should be pointed out that ε is very small, of the order of a fraction of percent.

The most striking result pertaining to eq. (7) is, undoubtedly, the possibility of stochastic resonance¹⁰⁾ : when $\Delta U_a \approx \Delta U_b$ and the forcing period, $2\pi/\omega$ is of the order of the characteristic passage times $\tau_{a,b}$ the response of the system is dramatically amplified. Specifically, the probability of crossing the barrier is sub-

stantially increased and the passage occurs with a periodicity equal to the periodicity of the forcing. This allows us to understand, at least qualitatively, how despite its weakness a periodic forcing may leave a lasting signature in the climatic record.

The interest of the description outlined in this section lies in its generality. Whatever the detailed features of a system might be, we know that near a simple bifurcation point (pitchfork or limit point), the dynamics will reduce to a universal form involving only a few parameters. It is therefore tempting to develop a modelling whereby these parameters are first tuned to reproduce some known properties (like for instance the past record), and subsequently are used to make predictions about the future evolution.

3. CLIMATIC VARIABILITY AND SUSTAINED OSCILLATIONS

Our next step will be to account for the cyclic character of long term climatic changes like quaternary glaciations in a more straightforward manner. Indeed, according to the theory of dynamical systems, one-dimensional attractors in the form of limit cycles can account for periodic, sustained oscillations. Let us therefore explore the possibilities afforded by oscillatory climate models.

Large parts of the chapters by Ghil⁵⁾ and Saltzman⁶⁾ are devoted to the derivation of such models. Here, we shall first adopt a more general viewpoint, and use later on these models to illustrate the basic ideas.

Suppose that oscillatory behavior arises through a Hopf bifurcation, leading from a hitherto stable steady state to a self-oscillation of the limit cycle type⁴⁾. We know that a dynamical system operating in the vicinity of such a bifurcation can be cast in a universal, normal form. Specifically, there exists a suitable linear (generally complex-valued) combination of the initial variables obeying to the equation¹¹⁾

$$\frac{dz}{dt} = (\lambda + i\omega_0) z - cz |z|^2 \quad (8)$$

Here t is a dimensionless time, λ the distance from the bifurcation point, ω_0 the frequency of the linearized motion around the steady state, and $c = u + iv$ a combination of the other parameters occurring in the initial equations. In Appendix A a detailed illustration of the process of reduction to a normal form is provided, using Saltzman's model oscillator describing the interaction between sea-ice extent and mean ocean temperature⁶⁾.

Coming back to the normal form, eq. (8), we switch to radial and angular variables through

$$z = r e^{i\varphi} \quad (9)$$

Substituting into (8) we readily verify that the evolution can be separated into a radial part, which is independent of φ , and an angular part depending solely on r :

$$\frac{dr}{dt} = \lambda r - ur^3 \quad (10a)$$

$$\frac{d\varphi}{dt} = \omega_0 - vr^2 \quad (10b)$$

The first of these equations allows us to evaluate analytically the radius of the limit cycle. Setting $dr/dt = 0$, which in the (r, φ) representation places us on the limit cycle, we obtain :

$$r_s = \left(\frac{\lambda}{u} \right)^{1/2} \quad (11a)$$

This solution exists provided that λ/u is positive. To test its stability we study the evolution of a small perturbation $\delta\rho = r - r_s$. Linearizing eq. (10a) around r_s , by virtue of the theorem of linearized stability (see chapter by G. Nicolis⁴), one obtains :

$$\begin{aligned} \frac{d\delta\rho}{dt} &= (\lambda - 3ur_s^2) \delta\rho \\ &= -2\lambda \delta\rho \end{aligned} \quad (11b)$$

As long as $\lambda > 0$ (and thus automatically $u > 0$ also) this predicts an exponential relaxation to the limit cycle. In other words the variable r enjoys in this range asymptotic stability, in the sense that any perturbation that may act accidentally on r will be damped by the system.

The situation is entirely different for φ . Setting r equal to its value on the limit cycle, which is legitimate in the limit of long times (and provided of course that $\lambda > 0$, $u > 0$), one can integrate eq. (10b) straightforwardly to get

$$\varphi = \varphi_0 + \left(\omega_0 - \frac{\lambda v}{u} \right) t \quad (11c)$$

In other words φ increases continuously in the interval $(0, 2\pi)$ from the initial value φ_0 . If φ_0 is perturbed, this monotonic change will start all over again from the new value, and there will be no tendency to reestablish the initial phase φ_0 ¹².

In order to realize more fully the consequences of this property let us consider the following thought experiment (Fig. 4) Suppose that the system runs on its limit cycle $r = r_s$. At some moment, corresponding to a value $\varphi = \varphi_1$ of the phase, we displace the system to a new state characterized by the values r_0, φ_0 of the variables r and φ . According to eq. (11b) the variable r will relax from r_0 back to the value r_s , as the representative point in phase space will spiral toward the limit cycle (cf. Fig. 4). On the other hand, according to eq. (11c) the phase variable φ will keep forever the memory of the initial value φ_0 . In other words, when the limit cycle will be reached again, the phase will generally be different from the one that would characterize an unperturbed system following its limit

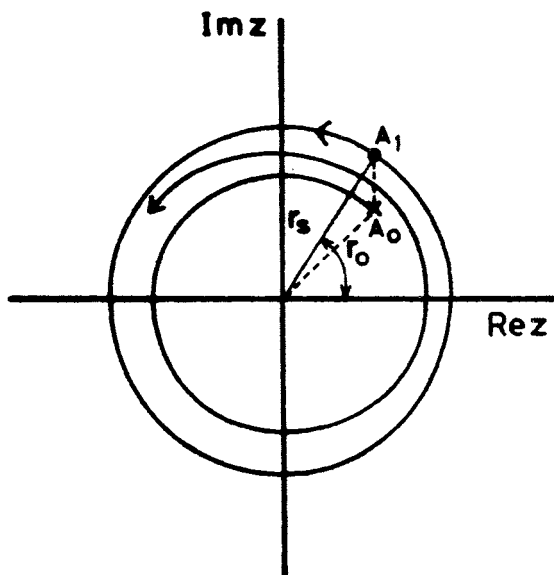


Fig. 4. Schematic representation of the evolution following the action of a perturbation leading from state A_1 on the limit cycle to state A_0 , in the space of the variables of the normal form.

cycle during the same time interval. In as much as the state into which the system can be thrown by a perturbation is unpredictable, it therefore follows that the reset phase of the oscillator will also be unpredictable. In other words, our non-linear oscillator is bound to behave sooner or later in an erratic way under the action of perturbations. This is tantamount to poor predictability.

The above surprising property can be further substantiated by a stochastic analysis. As stressed repeatedly in this Institute complex physical systems possess a universal mechanism of perturbations generated spontaneously by the dynamics, namely the fluctuations¹²⁾. Basically, fluctuations are random events. By modelling them as Gaussian white noises one is led to an augmented equation (8) in which the normal form variable z becomes itself a random process. The explicit form of this equation for Saltzman's model oscillator and its asymptotic solution are given in Appendix B. Here we summarize the most representative results.

i) one shows that the separation of the radial and phase variables is reflected, at the stochastic level, by the factorization

of the probability distribution. In the limit of long times one obtains a stationary distribution,

$$P(r, \varphi) = P(\varphi/r) P(r) = \frac{1}{2\pi} P(r) \quad (12)$$

ii) While the distribution of the phase variable is flat, the radial distribution $P(r)$ has the form

$$P(r) \sim \exp \left\{ -\frac{2}{Q} U(r) \right\} \quad (13a)$$

where Q is an effective variance of fluctuations and $U(r)$ is the potential associated with the right hand side of eq. (10a) :

$$U(r) = -\left(\lambda \frac{r^2}{2} - u \frac{r^4}{4} \right) \quad (13b)$$

It follows that φ is "chaotic", in the sense that the dispersion around its average will be of the same order as the average value itself. On the other hand, the dispersion of the radial variable around its most probable value is small, as long as the variance Q is small. Nevertheless, the mere fact that the probability of r is stationary rather than time-periodic implies that a remnant of the chaotic behavior of φ subsists in the statistics of r : if an average over a large number of samples (or over a sufficient time interval in a single realization of the stochastic process) is taken, the periodicity predicted by the deterministic analysis will be wiped out as a result of destructive phase interference¹²⁾.

In short, an autonomous oscillator cannot leave a marked signature on the long term climatic record : We have to look elsewhere to find an explanation of climatic changes believed to present a cyclic character, like the quaternary glaciations.

We shall now outline the analysis of a climatic oscillator forced by a weak periodic perturbation simulating, for instance, the earth's orbital variations. We shall show that under certain conditions, a stabilization of the phase of the oscillator can take place. This will remove unpredictability and guarantee the subsistence of periodic behavior over arbitrarily long times.

We shall illustrate this possibility by assuming the forcing to be additive. This is indeed the case for Saltzman's model as shown in Appendix C where further explicit results on the effect of forcing on this particular oscillator are outlined. The normal form, eq. (8) now reads¹³⁾ :

$$\frac{dz}{dt} = (\lambda - i\omega_0) z - cz|z|^2 + \varepsilon s \cos \omega_e t \quad (14)$$

Here $2\pi/\omega_e$ is the external periodicity, ε an effective forcing amplitude assumed to be small, and s a complex-valued coefficient describing the coupling of the forcing with the normal form variable.

It will prove convenient to work with the equations for the real and imaginary parts of our variable z . Setting

$$z = x + iy \quad , \quad s = s_x + is_y$$

we obtain from eq. (14) :

$$\begin{aligned}\frac{dx}{dt} &= \lambda x - \omega_0 y - (ux - vy) (x^2 + y^2) + \varepsilon s_x \cos \omega_e t \\ \frac{dy}{dt} &= \omega_0 x + \lambda y - (vx + uy) (x^2 + y^2) + \varepsilon s_y \cos \omega_e t\end{aligned}\quad (15)$$

A rather elaborate argument, which is not reproduced here, shows that phase stabilization - the phenomenon we are looking for - cannot be expected unless the system is in the immediate vicinity of bifurcation ($\lambda = 0$) and resonance ($\omega_0 = k\omega_e$, k integer). Now, in this range standard perturbation techniques fail (see also reference¹⁷). The following singular perturbation scheme seems to satisfy all requirements. First, we express the vicinity of bifurcation and resonance through

$$\lambda = \bar{\lambda} \varepsilon^{2/3}, \quad \omega_e - \omega_0 = \bar{\omega} \varepsilon^{2/3} \quad (16a)$$

Next, we introduce a fast time scale adjusted to the external forcing ($T = \omega_e t$) and a slow one ($\tau = \varepsilon^{2/3} t$) accounting for resonance :

$$\frac{d}{dt} = \omega_e \frac{d}{dT} + \varepsilon^{2/3} \frac{d}{d\tau} \quad (16b)$$

Finally, we expand x and y in perturbation series as follows :

$$\begin{aligned}x &= \varepsilon^{1/3} x_1 + \varepsilon^{2/3} x_2 + \varepsilon x_3 + \dots \\ y &= \varepsilon^{1/3} y_1 + \varepsilon^{2/3} y_2 + \varepsilon y_3 + \dots\end{aligned}\quad (16c)$$

Substituting into eqs (15) we obtain, to order $\varepsilon^{1/3}$, a homogeneous system of equations :

$$\frac{dx_1}{dT} = -y_1, \quad \frac{dy_1}{dT} = x_1 \quad (17)$$

whose solution is a harmonic oscillation :

$$\begin{aligned}x_1 &= A(\tau) \cos T + B(\tau) \sin T \\ y_1 &= A(\tau) \sin T - B(\tau) \cos T\end{aligned}\quad (18)$$

The integration coefficients A , B remain undetermined at this stage, They are expected to depend on the slow time scale τ which has not entered in eqs (17). To fix this dependence we consider the perturbation equations to the subsequent orders. As seen more explicitly in Appendix C these equations are now inhomogeneous. In order that they admit non-singular solutions we must make sure that certain solvability conditions are satisfied which, roughly speaking, guarantee that there is no risk of dividing a finite expression by zero¹⁸). For the problem under consideration there are two such solvability conditions which provide us with the following set of equations for the coefficients A and B :

$$\begin{aligned}\frac{dA}{d\tau} &= \bar{\lambda}A - \bar{\omega}B - (uA + vB)(A^2 + B^2) + \frac{s}{2}x \\ \frac{dB}{d\tau} &= \bar{\omega}A + \bar{\lambda}B + (vA - uB)(A^2 + B^2) - \frac{s}{2}y\end{aligned}\quad (19)$$

These equations can admit up to three real steady-state solutions which, by eqs (18), correspond to time-periodic solutions of the original system oscillating in resonance with the forcing. More importantly, since A and B are given once the parameters are specified, the phase of this oscillation relative to the forcing is well-defined¹³⁾. We have thus succeeded in reestablishing predictability thanks to this phase-locking phenomenon. Naturally, in order that phase-locking be physically relevant we must make sure that it corresponds to a stable solution of eqs (19). This is indeed so in a certain range of parameter values. On the other hand, beyond this range eqs (19) may give rise to a Hopf bifurcation for A and B. According to eqs (18) this corresponds to quasi-periodic solutions of the original system. The phase of the system relative to the forcing will now be a complicated function of time, and this will result in a rather loose predictability.

As in the preceding section, the interest of the description based on the normal form lies in its generality. For instance, ω_0 , ω_e and s in eq. (14) can be tuned to the values suggested by the record and the astronomical theory, while parameters λ and c are related to the amplitude of the oscillation. If information on this latter quantity is available, eq. (14) can then be used to study different scenarios concerning, for instance, the effect of disturbances of various kinds on the evolution.

4. CLIMATIC VARIABILITY AND NON-PERIODIC BEHAVIOR

Let us contemplate once again the climatic record, Figs 1 and 2. We see a broad band structure, in which an appreciable amount of randomness is superimposed on a limited number of preferred peaks. So far the broad band aspect was discarded in our discussion. We now raise the question, whether it could not be accounted for by dynamical regimes more complex than the phase locked one analyzed in the previous section. As a byproduct such regimes could still lead to distinct peaks in some preferred frequencies, but this would by no means imply that the behavior is periodic in time. The question we have just raised will lead us to examine a class of oscillatory models in which the coupling with the external forcing introduces a completely aperiodic behavior^{19,20)}.

The normal form of a periodically forced oscillator in the vicinity of a Hopf bifurcation (eqs (14) - (15)) cannot account for this type of solution^{12,13)}. On the other hand in the theory of dynamical systems one shows that such a behavior can arise near parameter values for which the system admits very special orbits known as homo-

clinic orbits, a flavor of which is given in the chapter by G.Nicolis⁴⁾ Fig. 5 depicts a typical phase space portrait of a two-variable dynamical system involving a pair of homoclinic orbits. We observe two stable fixed points $(x_a, 0)$ and $(x_b, 0)$ around which the system

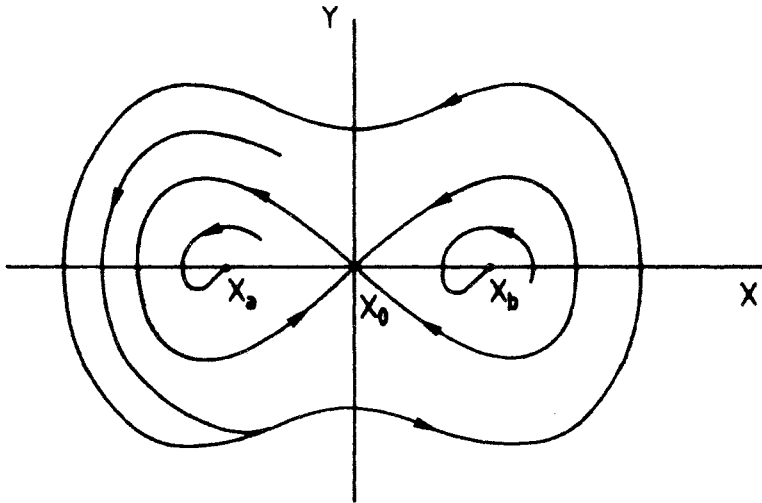


Fig. 5. Phase space portrait of a two variable system involving a pair of homoclinic orbits.

performs damped oscillations. An intermediate unstable point $(x_0 = 0, 0)$ gives rise to a pair of unstable and a pair of stable trajectories known as separatrices, which eventually merge to form the double loop structure. These are precisely our homoclinic trajectories, which can also be viewed as infinite period orbits. Further away in phase space the system admits a large amplitude stable periodic solution of finite period.

As an illustration of the phase space portrait of Fig. 5 consider Saltzman's oscillator (see chapter by Saltzman⁶⁾ and Appendices A to C). One has, in dimensionless variables,

$$\begin{aligned} \frac{d\eta}{dt} &= \theta - \eta \\ \frac{d\theta}{dt} &= b\theta - a\eta - \eta^2\theta \end{aligned} \quad (20)$$

where η and θ are, respectively, the (suitably scaled) deviations of the sine of latitude of sea ice extent and of the mean ocean temperature from a reference state. The system given by eqs. (20) may admit up to three steady states $(\theta'_s = \eta'_s = 0 \text{ and } \theta'_s = \eta'_s = \pm(b-a)^{1/2})$.

The linearized equations (20) around the trivial state ($\eta = \eta_s + \delta\eta$, $\theta = \theta_s + \delta\theta$) are simply

$$\begin{aligned}\frac{d\delta\eta}{dt} &= \delta\theta - \delta\eta \\ \frac{d\delta\theta}{dt} &= b\delta\theta - a\delta\eta\end{aligned}$$

They admit solutions which depend on time exponentially, with an exponent given by the characteristic equation (see chapter by G. Nicolis⁴)

$$\omega^2 - \omega(b - 1) + a - b = 0 \quad (21)$$

When $a > b$ and $b = 1$ this equation admits a pair of purely imaginary solutions. For $b > 1$ and $a > b$ the real part becomes positive^{12,13}. This is the range of Hopf bifurcation, which was discussed extensively in Section 3. On the other hand for $a < b$ the characteristic equation admits two real solutions of opposite sign. The reference state ($\theta = \eta_s = 0$) behaves then as a saddle, just like ($x_0 = 0, 0$) in Fig. 5. Both kinds of regimes merge for $a = b$, $b = 1$ for which values both roots of the characteristic equation vanish simultaneously.

We now set

$$\theta - \eta = \xi \quad (22)$$

Substituting into eqs. (20) we obtain

$$\begin{aligned}\frac{d\eta}{dt} &= \xi \\ \frac{d\xi}{dt} &= (b - 1)\xi + (b - a)\eta - \eta^3 - \eta^2\xi\end{aligned} \quad (23)$$

Near the degenerate situation in which both characteristic roots vanish simultaneously one has

$$\begin{aligned}b - 1 &= \varepsilon_1 \ll 1 \\ b - a &= \varepsilon_2 \ll 1\end{aligned} \quad (24)$$

It can be verified that for $\varepsilon_1 = 0.8 \varepsilon_2$ eqs (23) generate the phase portrait of Fig. 5. As a matter of fact eqs (23) are no less than the normal form of any dynamical system operating near the degenerate situation in which both characteristic roots vanish simultaneously¹⁹. The validity of our conclusions extends therefore far beyond the specific model of eqs (20).

We now study the coupling between the above defined system and a weak periodic forcing. To simplify as much as possible we consider an additive periodic forcing acting on the second equation (23) alone :

$$\frac{d\eta}{dt} = \xi$$

$$\frac{d\xi}{dt} = \varepsilon_1 \xi + \varepsilon_2 \eta - \eta^3 - \eta^2 \xi + s \sin \omega t \quad (25)$$

where s and ω are, respectively, the amplitude and the frequency of the forcing. We perform the following scaling of variables and parameters :

$$\begin{aligned} \eta &= x\mu & , \quad \xi &= y\mu^2 & , \quad s &= p\mu^4 \\ \varepsilon_1 &= \gamma_1 \mu^2 & , \quad \varepsilon_2 &= \gamma_2 \mu^2 & , \quad \mu &\ll 1 \\ t &= \tau \mu^{-1} & , \quad \omega &= \Omega \mu \end{aligned} \quad (26)$$

Eqs (25) become

$$\begin{aligned} \frac{dx}{d\tau} &= y \\ \frac{dy}{d\tau} &= \gamma_2 x - x^3 + \mu(\gamma_1 y - x^2 y + p \sin \Omega \tau) \end{aligned} \quad (27)$$

These equations can be viewed as the perturbations (for $\mu \ll 1$) of a reference system described by

$$\begin{aligned} \frac{dx_0}{d\tau} &= y_0 \\ \frac{dy_0}{d\tau} &= \gamma_2 x_0 - x_0^3 \end{aligned} \quad (28)$$

Remarkably, this is a Hamiltonian system known as Duffing's oscillator¹⁹⁾. For $\gamma_2 > 0$ its phase portrait is depicted in Fig. 6. We now have a continuum of periodic trajectories as well as a pair of homoclinic orbits existing for all positive values of the parameter γ_2 . Going from eqs (28) to eqs (27) amounts therefore to inquiring how this phase space structure and, in particular, the infinite period homoclinic orbits are perturbed by both the "dissipative" terms $\gamma_1 y - x^2 y$ and by the periodic forcing.

Let us first formulate this problem analytically. Setting $x = x_0 + \mu u$, $y = y_0 + \mu v$, we obtain the following equations for the perturbations u , v :

$$\begin{aligned} \frac{du}{d\tau} &= v \\ \frac{dv}{d\tau} &= (\gamma_2 - 3x_0^2)u + \gamma_1 y_0 - x_0^2 y_0 + p \sin \Omega \tau \end{aligned} \quad (29)$$

We now are in a situation similar to that arising in the perturbative

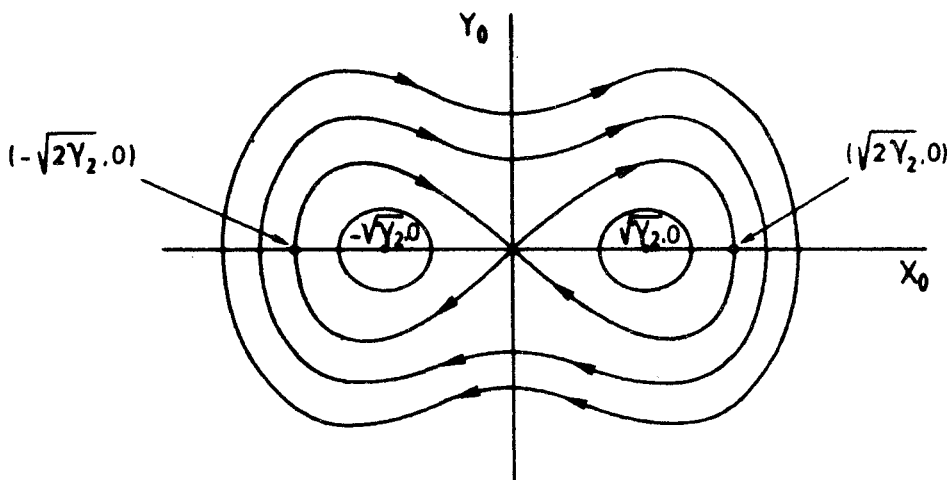


Fig. 6. Phase space portrait of Duffing's oscillator for $\gamma_2 > 0$.

analysis of eqs (15) : we have an inhomogeneous system of equations, which admits a non-singular solution provided that a solvability condition is satisfied. The argument is somewhat more elaborate than in Section 3 however, and will not be reproduced. We merely give the final result, known as Melnikov integral²¹⁾ :

$$\int_{-\infty}^{\infty} dt y_0 [\gamma_1 y_0 - x_0^2 y_0 + p \sin \Omega t] = 0 \quad (30)$$

This relation allows us to identify a critical forcing amplitude, p_c beyond which the homoclinic orbit is destroyed by the periodic perturbation. One obtains, after a lengthy calculation²²⁾ :

$$p_c = \frac{1}{3} \gamma_2^{3/2} (\gamma_1 - \frac{4}{5} \gamma_2) \frac{\text{Ch} \frac{\Omega \pi}{(2\gamma_2)^{1/2}} + 1}{\text{Ch} \frac{\Omega \pi}{2(2\gamma_2)^{1/2}}} \quad (31)$$

In the theory of dynamical systems one shows that for $p > p_c$ a variety of complex non-periodic behaviors may arise²⁰⁾. In order to identify the nature of these regimes we turn to numerical simulations.

As stressed by other authors in this book, the most unambiguous way to characterize the type of regime displayed by a dynamical system is to study the evolution of a trajectory starting from a point in phase space.

cal system is to perform a Poincaré surface of section. Remember that we are dealing with a forced system involving the two variables x and y . Effectively, such a dynamics takes place in a three-dimensional space, since one can always express the forcing through $b\sin\chi_e$, $d\chi_e/dt = \Omega$, thereby introducing its phase χ_e as a third variable. One can now map the original continuous dynamical system into a discrete time system by following the points at which the trajectories cross (with a slope of prescribed sign) the plane $\cos_e = C$, corresponding to a given value of the forcing. One obtains, in this way a Poincaré map (Fig. 7) that is to say, a recurrence relation

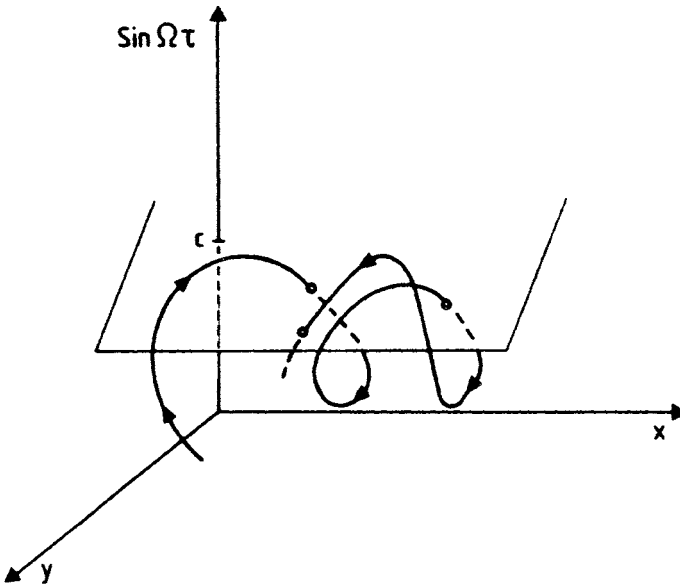


Fig. 7. Schematic representation of a Poincaré map for a forced system. As the system evolves, a representative trajectory cuts a plane of section C at discrete times τ_n . The study of the dynamics on the surface of the section gives valuable information of the qualitative behavior of the initial system.

$$\begin{aligned} x_{n+1} &= f(x_n, y_n) \\ y_{n+1} &= g(y_n, y_n) \end{aligned} \quad (32)$$

where n labels the successive intersections.

Suppose now that the trajectories of the continuous time flow tend, as $\tau \rightarrow \infty$, to an asymptotic regime. In the three-dimensional

state space, this regime will be characterized by an invariant object, the attractor. The signature of this object on the surface of the section will obviously be an attractor of the discrete dynamical system, eq. (32). Conversely, from the existence of an attractor on the surface of the section, we can infer the properties of the underlying continuous time flow.

Figure 8 depicts the Poincaré surface of section for values of p near the threshold p_C of eq. (31). We observe the coexistence of two attractors: A periodic one, with a period three times as large as the forcing period; and a quasi-periodic one, represented in the full phase space by a two-dimensional toroidal surface.

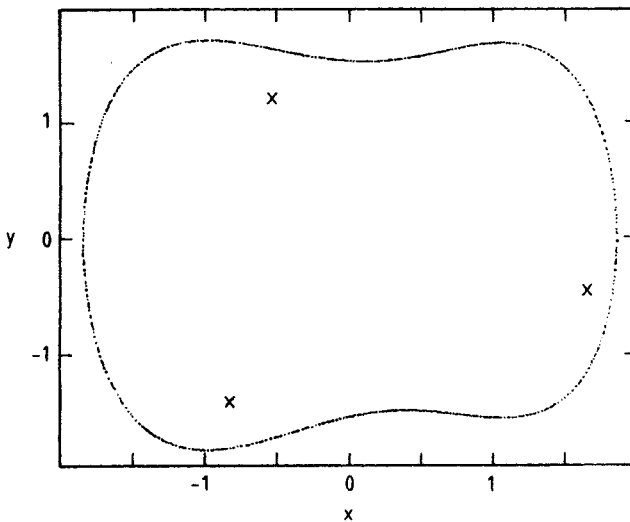


Fig. 8. Poincaré map of the forced system eqs. (27) for $\gamma_2 = 1$, $\gamma_1 = 1.01$, $\mu = 0.1$, $\Omega = 3$ and $q = q_C + 0.2$. Depending on the initial conditions the system evolves either to a quasi-periodic attractor (closed curve) or to a periodic one, with a period three times as large as the forcing period (points in crosses).

By increasing p further from p_C one observes the coexistence of two period three (Fig. 9a) and two period two attractors (Fig. 9b). As a matter of fact the attractors of a given period, differ by their phase relative to the phase of the forcing.

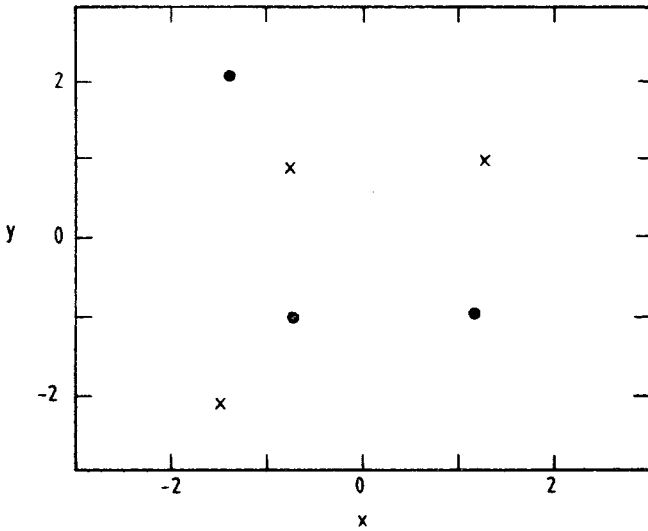


Fig. 9a. Poincaré map of the forced system eqs. (27) for the same parameter values as in Fig. 8 but with $q = 12q_0$. Note the coexistence of two different periodic attractors (points and crosses) with a period three times as large as the forcing period.

For still larger values of p the periodic attractors disappear, and a manifestly non-periodic stable regime dominates (Fig. 10a). We conjecture that we are in the presence of a chaotic attractor. This seems to be corroborated by the time dependence of the variables (Fig. 10b), as well as by the power spectrum, which exhibits an important broad band component along with a well-defined peak at the forcing frequency (Fig. 10c). More complex dynamical regimes which can be qualified as intermittent are also observed. For instance, after spending some time on a seemingly chaotic regime the system jumps on a period-three regime.

In short, we have identified an additional mechanism of climatic variability. The final question to which we now turn our attention is, which of the various regimes described in Sections 2 to 4 is best suited to interpret the climatic record?

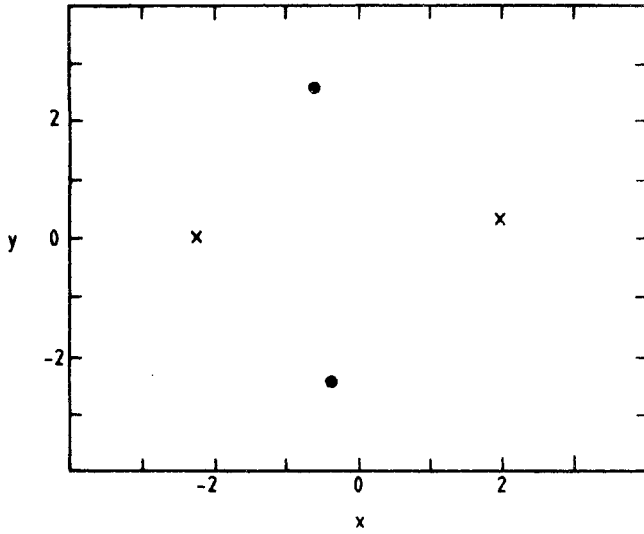


Fig. 9b. Same parameter values with Fig. 9a. Note the coexistence of two additional periodic attractors (points and crosses) with a period two times as large as the forcing period.

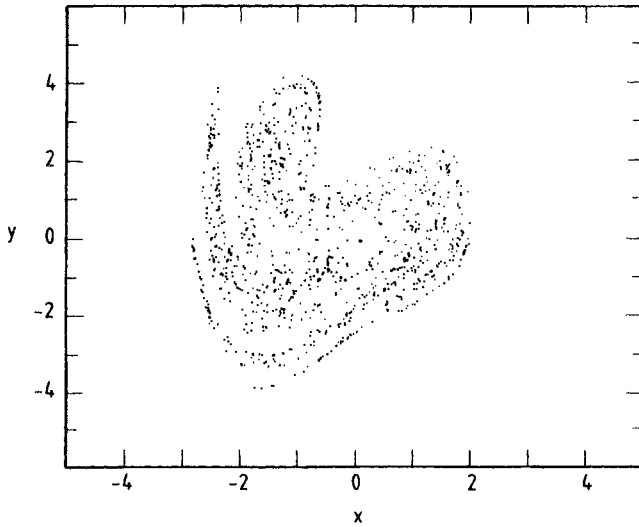


Fig. 10a. Non-periodic attractor of system (27) for the parameter values of Fig. 8 except $q = 20q_c$.

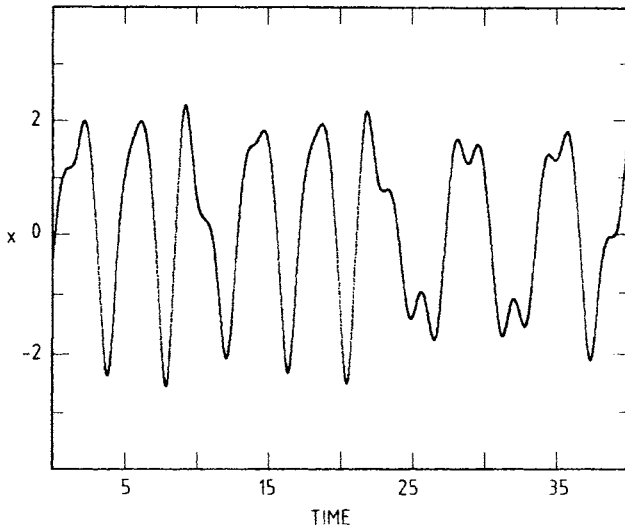


Fig. 10b. Time evolution of variable x for the parameter values used in Fig. 10a.

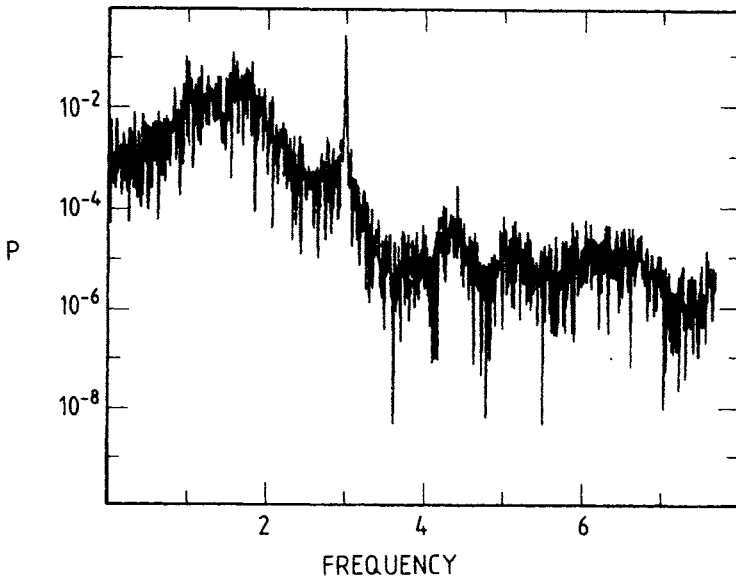


Fig. 10c. Power spectrum of the variable x whose time evolution is given in Fig. 10b.

5. RECONSTRUCTION OF THE CLIMATIC ATTRACTOR FROM TIME SERIES DATA

As pointed out in the Introduction much of our information on the climatic variability of the last million years is based on the oxygen isotope record¹⁾ (see Fig. 1). We will now show that it is possible to extract from such a record information going far beyond the traditional spectral analysis. In particular, we will be able to characterize the nature of the dynamical regime involved as well as to determine the minimum number of variables needed for its description²³⁾. We will illustrate this new method of data analysis on a particular deep-sea core known as V28-238.

Let $X_k(t)$ be the time series available from the data, and $X_k(t)$, where $k=0, 1, \dots, n-1$, the full set of variables actually taking part in the dynamics. X_k is expected to satisfy a set of first-order nonlinear equations^k, whose form is generally unknown but which, given a set of initial data $X_k(0)$, will produce the full details of the system's evolution.

By successive differentiations in time one can reduce this set to a single (generally highly nonlinear) differential equation of n th order in time for one of these variables. Thus instead of $X_k(t)$, $k = 0, 1, \dots, n-1$, we may consider $X_0(t)$, and its $n-1$ successive derivatives $X_0^{(k)}(t)$, $k = 1, \dots, n-1$, to be the n variables of the problem spanning the phase space of the system. Now, both $X_0(t)$ and its derivatives can be deduced from a single time series (the one for $X_0(t)$ as provided by the data). We see therefore that, as anticipated at the beginning of this section, we have in principle sufficient information in our disposal to go beyond the "one-dimensional" space of the original time series and to take into account the multi-dimensional character of the system's dynamics.

Actually, instead of $X_0(t)$ and $X_0^{(k)}(t)$ it will be easier to work with $X_0(t)$ and the set of variables obtained from it by shifting its values by a fixed lag τ ²⁴⁾. It suffices for this to choose τ in such a way that one keeps n linearly independent variables :

$$\begin{aligned}
 & X_0(t_1) \quad , \quad X_0(t_2), \dots \dots \dots X_0(t_N) \\
 & X_0(t_1+\tau) \quad , \quad X_0(t_2+\tau), \dots \dots \dots X_0(t_N+\tau) \\
 & X_0(t_1+(n-1)\tau), \quad X_0(t_2+(n-1)\tau) \dots \dots \dots X_0(t_N+(n-1)\tau)
 \end{aligned}
 \tag{33}$$

We will be interested in the structure of the trajectories of the dynamical system in the above defined phase space. The theory of dynamical systems shows that the structure of these trajectories is conditioned by two basic elements :

(i) The dimensionality of phase space, in other words, the number n of variables present.

(ii) The nature of the attractors, that is, of the asymptotically stable states attained in the course of time. The latter depends, in turn, on the dimensionality of the attractor.

A reference point \vec{X}_i from these data is now chosen and all its distances $|\vec{X}_i - \vec{X}_j|$ from the $N - 1$ remaining points are computed. This allows us to count the data points that are within a prescribed distance, r from point X_i . Repeating the process for all values of i , one arrives at the quantity

$$C(r) = \frac{1}{N^2} \sum_{\substack{i, j=1 \\ i \neq j}}^N \theta(r - |\vec{X}_i - \vec{X}_j|) \quad (34)$$

where θ is the Heaviside function, $\theta(x) = 0$ if $x < 0$, $\theta(x) = 1$ if $x > 0$. The non-vanishing of this quantity measures the extent to which the presence of a data point X_i , affects the position of the other points. $C(r)$ may thus be referred to as the (integral) correlation function of the attractor.

Suppose that we fix a given small parameter ϵ and we use it to define the site of a lattice which approximates the attractor. If the latter is a line, the number of data points within a distance r from a prescribed point should be proportional to r/ϵ . If it is a surface, this number should be proportional to $(r/\epsilon)^2$ and, more generally, if it is a d -dimensional manifold it should be proportional to $(r/\epsilon)^d$. We expect, therefore, that for r , relatively small $C(r)$ should vary as

$$C(r) = r^d \quad (35)$$

In other words, the dimensionality d of the attractor is given by the slope of the $\log C(r)$ versus $\log r$ in a certain range of values of r :

$$\log C(r) = d \log r \quad (36)$$

This property remains valid for attractors of fractal dimensionality.

The above results suggest the following algorithm :

(1) Starting from a time series, we can construct the correlation function, equation (34) by considering successively higher values of the dimensionality n of phase space.

(2) Deduce the slope d near the origin according to equation (36) and see how the result changes as n is increased.

(3) If d reaches a saturation limit beyond some relatively small n , the system represented by the time series should possess an attractor. The saturation value d_s will be regarded as the dimensionality of the attractor. The value of n beyond which saturation is observed will provide the minimum number of variables necessary to model the behavior represented by the attractor.

This procedure has been applied to the analysis of the data pertaining to core V28-238. Figure 12 gives the dependence of $\log C(r)$ versus $\log r$ for $n = 2$ to $n = 6$. We see that there is indeed an extended region over which this dependence is linear, in accordance with equation (36). Figure 13 (points in circles) shows that the slope

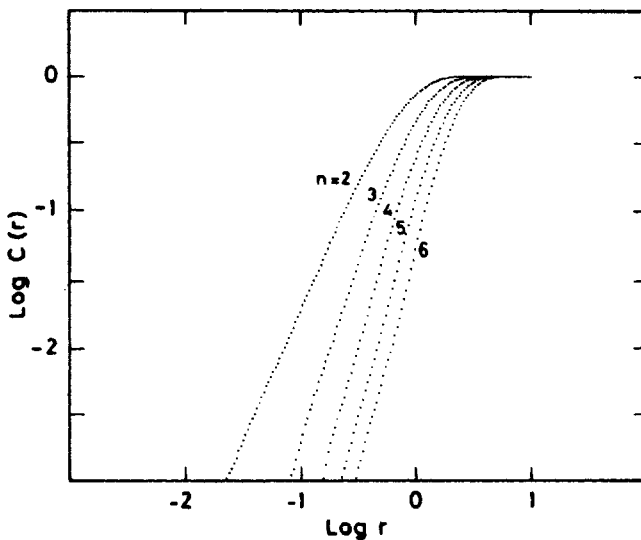


Fig. 12. Distance dependence of the correlation function on the climatic attractor. Parameter values as in Fig. 11, except that $\tau = 4 \Delta t$.

reaches a saturation value at $n = 4$, which is about $d_s = 3.1$. The same plot also shows the way in which d varies with n if the signal considered is a Gaussian white noise: there is no tendency to saturate. In fact, in this case d turns out to be equal to n . It should be emphasized that the above results are independent of the choice of the time lag τ , provided that the latter is of the order of magnitude of the time scales pertaining to the long-term climatic evolution, and the linear independence of the variables is secured.

The existence of a climatic attractor of low dimensionality shows that the main features of long-term climatic evolution may be viewed as the manifestation of a deterministic dynamics, involving a limited number of key variables. The fact that the attractor has a fractal dimensionality provides a natural explanation of the intrinsic variability of the climatic system, despite its deterministic character²⁶). Moreover, it suggests that despite the pronounced peaks of spectra in the frequencies of the orbital forcings, the actual behavior is highly non periodic⁵).

This last aspect was further substantiated by the estimation of the largest positive Lyapounov exponent⁴). We know that there exist as many Lyapounov exponents as phase space dimensions. In this particular case this number is four. One of them is necessary equal to zero expressing the fact that the relative distance of initially close

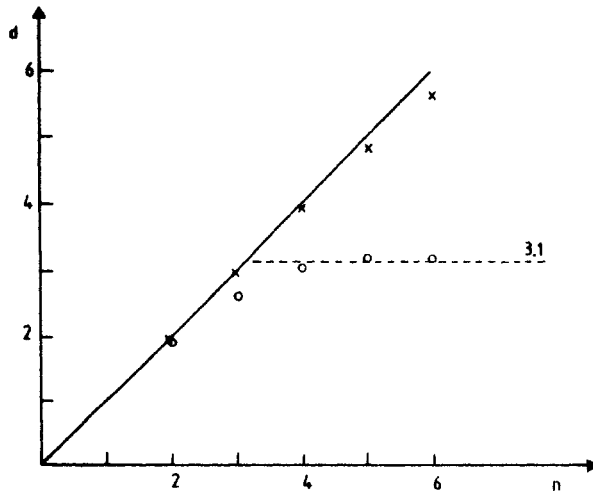


Fig. 13. Dependence of dimensionality, d on the number of phase space variables n , for the climatic attractor (O) and for a white noise signal (x) for the same parameter values as in Fig. 12.

states on a given trajectory varies slower than exponentially. Others are negative, expressing the exponential approach to the attractor. Finally, if the dynamics is chaotic, there will be at least one positive Lyapounov exponent witnessing the exponential divergence of nearby initial conditions on the stable attractor. Clearly, such a quantity is the ideal tool for describing the limits of predictability in climatic change. Note that in a well-behaved dissipative system the sum of all Lyapounov exponents must be strictly negative⁴⁾.

Recent algorithms²⁷⁾ allow for the calculation of the largest positive Lyapounov exponent of a dynamical system from time series data. We have applied this procedure to the data set of Fig. 1 and found indeed a positive number σ , between 2.5×10^{-5} and 4×10^{-5} yr^{-1} . Its inverse, σ^{-1} , between 25 and 40 kyr gives the limits of predictability of the long term behavior of the system²⁸⁾.

A further characterization of the nature of the underlying dynamical system is provided by the time correlation function of our data set. Figure 14 depicts this function. We observe a decay for small to intermediate times, a negative region and subsequently irregular oscillations around zero. This leads us to several important

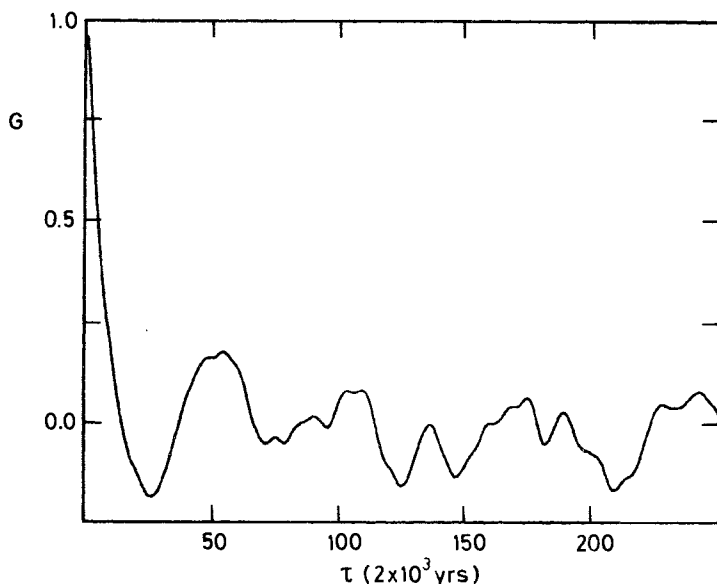


Fig. 14. Time correlation function of the variable X_0 on the climatic attractor.

conclusions. First, the fact that the correlation function is not merely periodic or quasi-periodic, proves that climate dynamics cannot be viewed as a passive response to the orbital forcings. Second, the fact that the correlation function decays for short to intermediate times proves that we are dealing with a process displaying unpredictability. Barring white noise, the simplest example of such a process is a Markovian red noise generated, for instance, by an Ornstein-Uhlenbeck process. If however this was the case here, the correlation function would never go to zero and would decay strictly exponentially. Neither of these two properties holds for Fig. 14. We conclude that we deal with a process possessing memory²⁸⁾. Moreover, the limits of predictability provided by the inverse of the largest positive Lyapounov exponent correspond, roughly, to a time in the interval between the vanishing and the first minimum of the correlation function. We believe therefore that we have produced strong evidence that long term climatic variability is to be viewed as a chaotic dynamics possessing a low dimensional attractor characterized by an unstable dynamics of limited predictability.

6. CONCLUDING REMARKS

The principal idea which we tried to convey in the present chapter is that dynamical systems theory provides us with new ways

to look at the long standing problem of climatic variability. For instance, modelling based on normal forms is a pragmatic tool for making rapid progress in problems involving a multitude of variables, which would remain otherwise intractable or would require extensive empirical parameterizations. Even more significant, perhaps, is the possibility to arrive at quantitative predictions of such quantities as attractor dimensions or predictability limits from time series data, independent of any modelling.

In the light of these possibilities problems related to intermediate and short range variability constitute a promising area of future investigations.

APPENDIX A

Consider Saltzman's model oscillator describing the interaction between sea-ice extent and mean ocean temperature¹⁴⁾

$$\begin{aligned} \frac{d\bar{\eta}}{dt} &= -\varphi_2 \bar{\eta} + \varphi_1 \bar{\theta} \\ \frac{d\bar{\theta}}{dt} &= -\psi_1 \bar{\eta} + \psi_2 \bar{\theta} - \psi_3 \bar{\eta}^2 \bar{\theta} \end{aligned} \quad (A1)$$

Here φ_1, ψ_1 are positive parameters, $\bar{\eta}$ is the deviation of the sine of the latitude of the sea-ice extent from the steady state and $\bar{\theta}$ is the excess mean ocean surface temperature. By performing the scaling transformation

$$\bar{\eta} = \left(\frac{\varphi_2}{\psi_3} \right)^{1/2} \eta, \quad \bar{\theta} = \frac{\varphi_2^{3/2}}{\psi_3^{1/2} \varphi_1} \theta, \quad \bar{t} = \frac{1}{\varphi_2} t \quad (A2)$$

we can cast eqs. (A1) in a form displaying two dimensionless parameters :

$$\begin{aligned} \frac{d\eta}{dt} &= -\eta + \theta \\ \frac{d\theta}{dt} &= -a\eta + b\theta - \eta^2 \theta \end{aligned} \quad (A3)$$

with

$$a = \frac{\psi_1 \varphi_1}{\varphi_2^2}, \quad b = \frac{\psi_2}{\varphi_2}$$

The procedure transforming eqs. (A3) to the normal form can now be outlined. We first compute the characteristic roots of the linearized stability problem. Straightforward algebra gives :

$$\lambda \pm i\omega_0 = \frac{1}{2} \left\{ b - 1 \pm [(b - 1)^2 - 4(a - b)]^{1/2} \right\} \quad (A4)$$

At $\lambda = 0$ the system undergoes a bifurcation beyond which a limit cycle

is expected to emerge. In general the full problem of exactly solving eqs (A3) in this range is intractable. We therefore limit ourselves to the case where $\lambda \ll 1$. To this end we cast the dynamics in a form corresponding to a full diagonalization of the linear part of eqs (A3). This is achieved by a linear transformation T , which in the present case is a 2×2 matrix whose columns are the two right eigenvectors of the matrix coefficients of the linear part of (A3). This transformation matrix T turns out to be

$$T = \begin{pmatrix} 1 & 1 \\ \lambda + i\omega_0 + 1 & \lambda - i\omega_0 + 1 \end{pmatrix} \quad (A5)$$

Operating on both sides of (A3) with the inverse matrix T^{-1} and introducing the new (complex) variables

$$\begin{pmatrix} z \\ z^* \end{pmatrix} = T^{-1} \begin{pmatrix} \eta \\ \theta \end{pmatrix} \quad (A6)$$

or more explicitly

$$\begin{aligned} \eta &= 2 R_e z \\ \theta &= 2 (R_e z - \omega_0 \text{Im}z) \end{aligned} \quad (A7)$$

we obtain to the dominant order in λ , the following equation for the transformed variable z :

$$\frac{dz}{dt} = (\lambda + i\omega_0) z + \frac{i}{2\omega_0} (3 + i\omega_0) z |z|^2 \quad (A8)$$

giving rise to a radial and angular part of the form of eqs (10a) and (10b) respectively with $u = 1/2$ and $v = -3/(2\omega_0)$.

APPENDIX B

Let us incorporate the effect of fluctuations by adding random forces F_η , F_θ to the deterministic Saltzman oscillator¹⁴, eqs (A3) :

$$\begin{aligned} \frac{d\eta}{dt} &= -\eta + \theta + F_\eta \\ \frac{d\theta}{dt} &= -a\eta + b\theta - \eta^2\theta + F_\theta \end{aligned} \quad (B1)$$

Repeating the procedure given in Appendix A, transforming eqs (B1) to the normal form we obtain :

$$\frac{dz}{dt} = (\lambda + i\omega_0) z + \frac{i}{2\omega_0} \left\{ (3 + i\omega_0) z |z|^2 + (1 - i\omega_0) F_\eta - F_\theta \right\} \quad (B2)$$

Setting $z = x + iy$, substituting into eq. (B2) and separating real and imaginary parts one gets :

$$\begin{aligned} \frac{dx}{dt} &= \lambda x - \omega_0 y - \frac{1}{2} (x^2 + y^2) (x + \frac{3}{\omega_0} y) + F_x \\ \frac{dy}{dt} &= \omega_0 x + \lambda y - \frac{1}{2} (x^2 + y^2) (y - \frac{3}{\omega_0} x) + F_y \end{aligned} \quad (B3)$$

where we have set $F_x = F_\eta/2$ and $F_y = (F_\eta - F_\theta)/2\omega_0$. We assume F_η, F_θ to define a multi-Gaussian white noise⁸⁾:

$$\begin{aligned} \langle F_\eta(t) F_\eta(t') \rangle &= q_\eta (t - t') \\ \langle F_\theta(t) F_\theta(t') \rangle &= q_\theta (t - t') \\ \langle F_\eta(t) F_\theta(t') \rangle &= q_{\eta\theta} (t - t') \end{aligned} \quad (B4)$$

This allows us to write a Fokker-Planck equation for the probability distribution of the climatic variables

$$\begin{aligned} \frac{\partial P}{\partial t} &= - \frac{\partial}{\partial x} \left\{ \lambda x - \omega_0 y - \frac{1}{2} (x^2 + y^2) (x + \frac{3}{\omega_0} y) \right\} \\ &\quad - \frac{\partial}{\partial y} \left\{ \omega_0 x + \lambda y - \frac{1}{2} (x^2 + y^2) (y - \frac{3}{\omega_0} x) \right\} \\ &\quad + \frac{q_x}{2} \frac{\partial^2 P}{\partial x^2} + \frac{q_y}{2} \frac{\partial^2 P}{\partial y^2} + q_{xy} \frac{\partial^2 P}{\partial x \partial y} \end{aligned} \quad (B5)$$

where q_x, q_y, q_{xy} are the variances of F_x and F_y .

In general eq. (B5) is intractable. However, the situation is greatly simplified if one limits the analysis to the range in which the normal form (eqs (10)) is valid.

To see this it is convenient to introduce polar coordinates $x = r \cos \varphi, y = r \sin \varphi$. Note that the latter transformation being nonlinear, one should take into account the subtleties of Ito-Stratonivitch calculus¹⁵⁾. One obtains after a lengthy calculation¹⁶⁾:

$$\begin{aligned} \frac{\partial P(r, \varphi, t)}{\partial t} &= - \frac{\partial}{\partial r} \left\{ \lambda r - \frac{1}{2} r^3 + \frac{1}{2r} Q_{\varphi\varphi} \right\} P \\ &\quad - \frac{\partial}{\partial \varphi} \left\{ \omega_0 + \frac{3}{2\omega_0} r^2 - \frac{1}{r^2} Q_{r\varphi} \right\} P \\ &\quad + \frac{1}{2} \left\{ \frac{\partial^2}{\partial r^2} Q_{rr} + 2 \frac{\partial^2}{\partial r \partial \varphi} \frac{Q_{r\varphi}}{r} + \frac{\partial^2}{\partial \varphi^2} \frac{Q_{\varphi\varphi}}{r^2} \right\} P \end{aligned} \quad (B6)$$

where

$$\begin{aligned} Q_{\varphi\varphi} &= q_x \sin^2 \varphi - 2q_{xy} \sin \varphi \cos \varphi + q_y \cos^2 \varphi, \\ Q_{r\varphi} &= - q_x \sin \varphi \cos \varphi + q_{xy} (\cos^2 \varphi - \sin^2 \varphi) \\ &\quad + q_y \sin \varphi \cos \varphi, \end{aligned}$$

$$Q_{rr} = q_x \cos^2 \varphi + 2q_{xy} \sin \varphi \cos \varphi + q_y \sin^2 \varphi, \quad (B7)$$

and q_x , q_y and q_{xy} are suitable linear combinations of q_η , q_θ , $q_{\eta\theta}$. To go further it is necessary to introduce a perturbation parameter in the problem. It is reasonable to choose it to be related to the weakness of the noise terms. Mathematically, we express this through the following scaling :

$$\begin{aligned} Q_{\varphi\varphi} &= \varepsilon \bar{Q}_{\varphi\varphi}, \\ Q_{r\varphi} &= \varepsilon \bar{Q}_{r\varphi}, \\ Q_{rr} &= \varepsilon \bar{Q}_{rr}, \end{aligned} \quad (B8)$$

We next scale both the bifurcation parameter λ and the deviation of the radius r from its value on the limit cycle, $r = r_s$, by suitable powers of ε . We do this in order to be in accordance with the conditions of validity of the normal form (eqs. (10)). However, we should keep in mind that the qualitative predictions should still describe the general trend beyond the vicinity of the bifurcation point. Note that no scaling can be applied to the angular variable φ , as the latter increases in the interval $(0, 2\pi)$ and does not enjoy any stability property. Summarizing we write¹⁶⁾ :

$$\begin{aligned} \lambda &= \bar{\lambda} \varepsilon^{2m} \\ r &= r_s + \rho \varepsilon^k = (2\bar{\lambda})^{1/2} \varepsilon^m + \rho \varepsilon^k \\ \varphi &= \varphi \end{aligned} \quad (B9)$$

The (non-negative) exponents k and m are chosen in such a way that both the drift and diffusion terms contribute to the evolution of P in eq. (B6). Indeed, should the diffusion terms be negligible, the probability P would be a delta function around the deterministic motion, and as a result the effect of fluctuations would be wiped out. If on the other hand the drift terms were negligible, P would exhibit a purely random motion similar to that of a Brownian particle in a fluid, and would tend to zero everywhere as $t \rightarrow \infty$. The best way to estimate the magnitude of these two terms is to introduce the conditional probability $P(\varphi/\rho, t)$ through

$$P(\rho, \varphi, t) = P(\varphi/\rho, t) P(\rho, t), \quad (B10)$$

where

$$P(\rho, t) = \frac{1}{2\pi} \int_0^{2\pi} d\varphi P(\rho, \varphi, t). \quad (B11)$$

Integrating eq. (B6) over φ and taking the scaling (B8) and (B9) into account, one can see that $\partial P(\rho, t)/\partial t$ is of order ε . $P(\rho, t)$ is therefore a slow variable : this is the probabilistic analogue of the fact

that the variable r varies at the slowest of all time scales present in the problem. Using this property and dividing through eq. (B6) with $P(\rho, t)$ we obtain a closed equation for $P(\varphi/\rho, t)$ which to dominant order in ε reads :

$$\frac{\partial P(\varphi/\rho, t)}{\partial t} = - \frac{\partial}{\partial \varphi} \omega_o P(\varphi/\rho, t) \tag{B12}$$

This equation admits a properly normalized stationary solution,

$$P(\varphi/\rho, t) = 1/(2 \pi). \tag{B13}$$

Introducing this into eq. (B10) and integrating eq. (B6) over φ , we can obtain a closed equation for the slow variable $P(\rho, t)$. From this equation one can see that the drift and diffusion terms are of the same order of magnitude if and only if

$$k = m = \frac{1}{4} \tag{B14}$$

The equation for $P(\rho, t)$ then reads :

$$\frac{\partial P(\rho, t)}{\partial t} = - \varepsilon^{1/2} \frac{\partial}{\partial \rho} \left[- 2\bar{\lambda}\rho - 3 \left(\frac{\bar{\lambda}}{2} \right)^{1/2} \rho^2 - \frac{1}{2} \rho^3 + \frac{\bar{Q}}{2(2\bar{\lambda}\varepsilon)^{1/2} + \rho} \right] P + \varepsilon^{1/2} \bar{Q} \frac{\partial^2}{\partial \rho^2} P \tag{B15}$$

where

$$\bar{Q} = \frac{1}{2} (q_x + q_y) . \tag{B16}$$

This equation admits a steady-state solution. Switching back to the original variables and parameters r , λ and Q through the inverse scaling (eqs. (B8) and (B9)), we can see that this steady-state is of the form

$$P_s(r) \sim r \exp \left\{ \frac{2}{Q} \left(\frac{\lambda r^2}{2} - \frac{r^4}{8} \right) \right\} \tag{B17}$$

APPENDIX C

14) Consider Saltzman's oscillator forced by a weak periodic forcing :

$$\begin{aligned} \frac{d\eta}{dt} &= - \eta + \theta + \varepsilon s_{\eta} \cos \omega_e t \\ \frac{d\theta}{dt} &= - a\eta + b\theta - \eta^2 \theta + \varepsilon s_{\theta} \cos \omega_e t \end{aligned} \tag{C1}$$

with $\varepsilon \ll 1$.

εs_1 , ω_e are respectively the dimensionless amplitudes of the forcing and its frequency. By applying the same procedure as in Appendix A the normal form of eqs (C1) is:

$$\frac{dz}{dt} = (\lambda + i\omega_0) z + \frac{i}{2\omega_0} \left\{ (3 + i\omega_0) z |z|^2 + \varepsilon [(1 - i\omega_0) s_\eta - s_\theta] \cos \omega_e t \right\} \quad (C2)$$

Setting $z = x + iy$ we obtain :

$$\begin{aligned} \frac{dx}{dt} &= \lambda x - \omega_0 y - \frac{1}{2} (x^2 + y^2) \left(x + \frac{3}{\omega_0} y \right) + \varepsilon s_x \cos \omega_e t \\ \frac{dy}{dt} &= \omega_0 x + \lambda y - \frac{1}{2} (x^2 + y^2) \left(y - \frac{3}{\omega_0} x \right) + \varepsilon s_y \cos \omega_e t \end{aligned} \quad (C3)$$

where we have set

$$s_x = \frac{s_\eta}{2}, \quad s_y = \frac{1}{2\omega_0} (s_\eta - s_\theta) \quad (C4)$$

We are interested in solving eqs (C4) in the case in which the system operates near the bifurcation point ($\lambda \ll 1$) and near resonance ($\omega_0 \sim \omega_e$). Following the singular perturbation scheme, eqs (16), one gets the solutions for the first order in the expansion x_1 and y_1 , given by eqs (18). The latter contain two unknown quantities A and B which may depend on the slow time scale τ .

The next order $\varepsilon^{2/3}$, leads to equations identical to (17) and therefore adds nothing new. To the order ε , on the other hand, we obtain :

$$\begin{aligned} \omega_e \left(\frac{\partial x_3}{\partial T} + y_3 \right) &= - \frac{\partial x_1}{\partial \tau} + \bar{\lambda} x_1 + \bar{\omega} y_1 \\ &\quad - \frac{1}{2} (x_1^2 + y_1^2) \left(x_1 + \frac{3}{\omega_0} y_1 \right) + s_x \cos T \\ \omega_e \left(\frac{\partial y_3}{\partial T} - x_3 \right) &= - \frac{\partial y_1}{\partial \tau} + \bar{\lambda} y_1 - \bar{\omega} x_1 \\ &\quad - \frac{1}{2} (x_1^2 + y_1^2) \left(y_1 - \frac{3}{\omega_0} x_1 \right) + s_y \cos T \end{aligned} \quad (C5)$$

This is an inhomogeneous system of equations for x_3 , y_3 . It admits a solution only if a solvability condition expressing the absence of terms growing unboundedly in time, is satisfied. Such terms may arise by the following mechanism. To obtain (x_3, y_3) , we have to "divide" the right-hand side of eqs. (C5) by the differential matrix operator

$$\omega_e \begin{pmatrix} \frac{\partial}{\partial T} & 1 \\ -1 & \frac{\partial}{\partial T} \end{pmatrix} \quad (C6)$$

but this is precisely the operator appearing in eqs. (17). According to this latter equation and eqs. (18), it possesses a non-trivial null space, that is, non-trivial eigenvectors corresponding to a zero eigenvalue. By dividing with such an operator, one may therefore introduce singularities, if the right-hand sides of eqs. (C5) contain contributions lying in this nul space. The solvability condition¹⁸⁾ allows one to rule out this possibility, by requiring that the right-hand sides of eqs. (C5) viewed as a vector, be orthogonal to the eigenvectors of the operator (C6). The latter are (cf. eq. (18)) :

$$(\cos T, \sin T) \quad \text{and} \quad (\sin T, -\cos T). \quad (C7)$$

The scalar product to be used is the conventional scalar product of vector analysis, supplemented by an averaging over T . The point is that we will dispose of two solvability conditions which will provide us with two equations for the coefficients $A(\tau)$, $B(\tau)$ appearing in the first order of the perturbative development (eqs. (18)). After a lengthy calculation one finds eqs. (19).

ACKNOWLEDGMENT

This work is supported, in part, by the European Economic Community under contract n° ST2J-0079-1-B (EDB).

REFERENCES

1. Shackleton, N.J. and Opdyke, N.D, *Quat. Res.* 3, 39-55 (1973).
2. Berger, A.L. and Pestiaux, P. Tech. Rep. N° 28, (Institute of Astronomy and Geophysics, Catholic University of Louvain, 1982).
3. Brock, W. and Chamberlain, G., SSRI W.P. n° 8419, Department of Economics, University of WI, Madison, WI (1984).
4. Nicolis, G. This volume.
5. Ghil, M. This volume.
6. Saltzman, B. This volume.
7. Crafoord, C. and Källén, E., *J. Atmos. Sci.* 35, 1123-1125 (1978).
8. Wax, N., Selected topics in noise and stochastic processes, New York, Dover (1954).
9. Nicolis, C. and Nicolis, G., *Tellus*, 33, 225-234 (1981).
10. Nicolis, C., *Tellus*, 34, 1-9 (1982).
Benzi, R., Parisi, G., Suter, A. and Vulpiani, A., *Tellus*, 34, 10-16 (1982).
11. Arnold, V., Chapitres supplémentaires de la théorie des équations différentielles ordinaires, Mir, Moscow (1980).
12. Nicolis, C., *Tellus*, 36A, 1-10 (1984).

13. Nicolis, C., *Tellus*, 36A, 217-227 (1984).
14. Saltzman, B., Sutera, A. and Hansen, A.R., *J. Atmos. Sci.*, 39, 2634-2637 (1982).
15. Arnold, L., Stochastic differential equations : Theory and applications, Wiley, New York (1974).
16. See also Baras, F., Malek-Mansour, M. and Van Den Broeck, C., *J. Stat. Phys.* 28, 577-587 (1982).
17. Rosenblat, S. and Cohen, D.S., *Stat. Appl. Math.*, 64, 143-175(1981).
18. Sattinger, D., Topics in stability and bifurcation theory, Springer-Verlag, Berlin (1973).
19. Guckenheimer, J. and Holmes, P., Nonlinear oscillations, dynamical systems and bifurcations of vector fields, Springer-Verlag, Berlin (1983).
20. Baesens, C. and Nicolis, G., *Z. Phys. B., Condensed Matter*, 52, 345-354 (1983).
21. Melnikov, V.K., *Trans. Moscow Math. Soc.* 12(1), 1-57 (1963).
22. Nicolis, C., *Tellus*, in press.
23. Nicolis, C. and Nicolis, G., *Nature*, 311, 529-532 (1984).
24. Ruelle, D. in Nonlinear phenomena in chemical dynamics, (eds Pacault A. and Vidal, C.), Springer, Berlin (1981).
25. See for instance, Grassberger, P. and Procaccia, I., *Phys. Rev. Lett.* 50, 346-349 (1983).
26. Lorenz, E.N., *Tellus*, 36A, 98-110 (1984).
Lorenz, E.N. This volume.
27. Wolf, A., Swift, J.B., Swinney, H.L. and Vastano, J.A., *Physica* 16D, 185 (1985).
28. Nicolis, C. and Nicolis, G., *Proc. Nat. Acad. Sci.*, in press.